International Journal of Pure and Applied Mathematics
Volume 78 No. 4 2012, 543-576
ISSN: 1311-8080 (printed version)
url: http://www.ijpam.eu

ijpam.eu

CALCULATION OF FLOWS OF A VISCOUS INCOMPRESSIBLE LIQUIDS BY MEANS OF ALGORITHMS OF THE RAISED ACCURACY

V.I. Kostin

Moscow State Academy of Water Transport
Block 1, Novodanilovskaya Enkh., 2
117105, Moscow, RUSSIAN FEDERATION

Abstract: This paper is devoted on the numerical simulations of incompressible stratified fluid. The implicit algorithm for solving the Navier-Stokes in Boussinesq approach equations based on the use of compact approximations of the third order for convective terms for equations is used. The diffusion terms of equations are approximated by the fourth order of accuracy. The results of the calculations are received.

AMS Subject Classification: 76-XX
Key Words: compact approximations, stratified medium, incompressible fluid

1. Introduction

From universal methods used for calculation of flows of an incompressible liquid during long time is method [1] and a lot of its modifications [2-4].

In a basis of the given algorithm of calculations for the equations introduced in variables of velocity vector - pressure, lays idea of pressure definition [2] (or corrections to pressure [3-5]) provided that on each time-layer the incompressibility condition $div\ \vec{v} = 0$ is true.

Received: June 4, 2012

Initial attempts of solutions reception have been connected with application of explicit algorithms where independent variables were calculated on new time layers [1-2]. However at carrying out of flows with small viscosity rigid restrictions on stability criterion of used algorithms led to increase of requirements to computers used.

One of the approaches, called up to weaken such requirements, is possible to consider application of implicit algorithms [3-7] possessing a greater range of stability. Other aspect by way of reception of satisfactory quality solution (with good properties of approximation and monotony) is the choice of appropriate approximation of the initial equations.

For this purpose often use the multipoint upwind operators [9] that leads to essential algorithm complication at use of implicit differenced schemes.

As alternative to it the implicit differenced scheme based on use of a compact upwind three-point operators for convective and diffusive terms approximation [10,4-8] is effective.

Its advantage consists that it possesses good dispersive and dissipation properties and has the high order of approximation: from the third and above [10-12], and a turning out system of the linear equations has the three-diagonal form which may be easily solved by sweep method [16].

So, in works [4-7] third order approximations for convective terms of the equations were applied, and diffusive ones were approximated with accuracy about O(h/Re). At wide ranges Reynolds's number such an approximation has appeared to be quite satisfactory [4,10], however at the problems solution of a general view approximation of higher order is required.

In work [8] the numerical algorithm based on approximation both convective, and diffusive terms of the equations with the third order of the accuracy, allowing investigations to be made over a wide range defining parameters of flows of a non-uniform incompressible liquid is realized.

In the present work the algorithm which contains approximation diffusion terms of the equations of the fourth order of accuracy is considered.

2. Statement of a Problem and the Basic Equations

The flow of completely mixed liquid in the stratified media within the frames of a viscous incompressible liquid with linear stratification of density (or temperatures) on depth is considered.

The problem in question is described by Navier-Stokes equations introduced for variables of velocity vector - pressure in Boussinesq approximation when

difference of media density from its not indignant value is considered only in forces of buoyancy.

Thus, the studied phenomenon is considered in the Cartesian system of coordinates $(O,\ x,\ y,\ z)$ or $(O,\ x_1, x_2, x_3)$, and the beginning of coordinates coincides with the center of the disturbed area. Axis Ox is directed along a stream, Oz - vertically upwards, and Oy supplements system of coordinates up to the right three.

The media stratification in undisturbed condition is defined by density distribution $\rho = \rho_0(z)$ (or temperature $T = T_0(z)$). It is well known that the stratification degree is characterized by Brent-Vaisala frequency defined by following equation

$$N^2 = -\frac{g}{\rho_*} \cdot \frac{\partial \rho_0}{\partial z}, \tag{2.1}$$

where $\rho_* = \rho_0(0)$, and g – free falling acceleration.

Let u_1, u_2, u_3 to denote a velocity vector $\overrightarrow{V}$ projections on appropriating axes of coordinates. According to [2-5,13,14] the viscous incompressible liquid flow is described by following system of the equations:

$$\frac{D\rho u_i}{Dt} = -\frac{\partial p}{\partial x_i} + \rho\nu\Delta u_i - \rho g_i. \tag{2.2}$$

$$\frac{\partial u_i}{\partial x_i} = 0. \tag{2.3}$$

Here:

$g_1 = g_2 = 0,\ g_3 = g$– free falling acceleration,

Δ - Laplace Operator,

$$\frac{Df}{Dt} - \text{ Full time derivative.}$$

In Boussinesq approximation the system of the equations (2.2) will become (2.4):

$$\frac{Du_i}{Dt} = -\frac{1}{\rho_*}\frac{\partial p}{\partial x_i} + \nu\Delta u_i - \frac{\rho}{\rho_*} g_i. \tag{2.4}$$

To define value of density ρit is necessary to add a following equation [3-5,15]

$$\frac{D(\rho - \rho_0)}{Dt} = -u_i \frac{\partial \rho_0}{\partial x_i}. \tag{2.5}$$

Thus, the investigated problem is solved within the frames of the equations (2.3) - (2.5). If L, U and L/U to choose as characteristic values of scales of length, speed and time of the considered phenomenon, in the equations (2.3) - (2.5) it is possible to pass to dimensionless values.

$$v_i = \frac{u_i}{U}, \quad y_i = \frac{x_i}{L}, \quad \tau = \frac{Ut}{L}. \tag{2.6}$$

Dimensionless density disturbance thus is entered under the formula

$$\bar{\rho} = \frac{\rho - \rho_0}{L\frac{\partial \rho_0}{\partial z}}. \tag{2.7}$$

The pressure is usually considered in the form of

$$\frac{\partial \pi}{y_i} = \frac{1}{\rho_*}\left(\frac{\partial p}{\partial y_i} + \rho_0 g_i\right). \tag{2.8}$$

Consequently, using the (2.6)-(2.8) formulas it is easy to receive the following equations:

$$\frac{\partial v_i}{\partial y_i} = 0, \tag{2.9}$$

$$\frac{Dv_i}{D\tau} = -\frac{\partial \pi}{\partial y_i} + \frac{1}{Re}\Delta v_i + \frac{\bar{\rho}}{Fr^2}\delta_{i3}, \tag{2.10}$$

$$\frac{D\bar{\rho}}{D\tau} = -v_i\delta_{i3}. \tag{2.11}$$

Here Reynolds's and Frud's dimensionless numbers are certain by following equations (N - Brent-Vaisala frequency (2.1)):

$$Re = \frac{UL}{\nu}, \quad Fr = \frac{U}{NL}. \tag{2.12}$$

As already it was mentioned above, the mixed liquid which area of hashing represents the infinite cylinder of radius $L$with forming - axis Ox is considered.

So, the non-stationary flow generated by a site of the mixed liquid ($y^2+z^2 \leq L^2$) is considered at availability of stable stratification $\rho = \rho_0(z)$ of undisturbed stream with Brent-Vaisala frequency (2.1).

In initial point in time the liquid is undisturbed, and the density inside of the mixed area ("spot") is constant:

$$v(0,y,z) = w(0,y,z) = 0, \quad \rho(0,y,z) = \rho_* = const. \tag{2.13}$$

For linear stratification it is true, that

$$\rho_0(z) = \rho_*(1 - \alpha z). \tag{2.14}$$

Consequently initially in time $\tau = 0$the liquid outside the "spot" is undisturbed and in this area $\bar{\rho} = 0$, but inside of "spot" (according to formulas (2.7), (2.13) - (2.14)) -$\bar{\rho}$ =-z:

$$\bar{\rho} = \begin{cases} 0\ ,\ when\ \ y^2 + z^2 \geq L^2, \\ -z,\ when\ y^2 + z^2 \leq L^2. \end{cases} \tag{2.15}$$

The pressure defined by the formula (2.8), thus is specified by integration of value $\bar{\rho}(y, z)$ so that it conformed to a hydrostatic parity in all region of calculations [3-5]

$$\pi(0, y, z) = \frac{1}{Fr^2} \int \bar{\rho}(y, z)\, dz. \tag{2.16}$$

Thus, the problem about evolution of "spot" in steadily stratified (2.14) media with entry conditions (2.13), (2.15) - (2.16) which is described by system of the equations (2.9) - (2.11) is stated.

3. Algorithm of the Decision

For the numerical solution of the received system of the equations (2.9) - (2.11) in computational region the uniform mesh is introduced ω_h with the units having coordinates $(t_m, y_i,\ z_j)$

$$\omega_h :\ \ t_m = (m-1)\,\tau; \quad y_i = (i-1)\,h_y; \quad z_j = (j-1)\,h_z. \tag{3.1}$$

Values of all functions entering into the considered equations, are specified in the nodes of a grid ω_h (3.1):

$$f_{ij}^m = f(t_m, y_i, z_j). \tag{3.2}$$

The solution of the specified system of the equations is based on definition of the correction to pressure from Poisson equation with some right hand side which turns out from an incompressibility condition $div\vec{V} = 0$ on each time-layer $t = t_m$ [3-5].

According to [3-5, 13-15] the equations (2.10) can be introduced in the form of:

$$\frac{\partial v_i}{\partial \tau} + \frac{\partial v_i v_k}{\partial y_k} = -\frac{\partial \pi}{\partial y_i} + \frac{1}{Re}\Delta v_i + \frac{\bar{\rho}}{Fr^2}\delta_{i3}. \tag{3.3}$$

If enter the operator

$$L\left(f_m\right)=\frac{\partial f_m v_k}{\partial y_k}-\frac{1}{Re}\Delta f_m-\frac{\bar{\rho}}{Fr^2}\delta_{m3}, \tag{3.4}$$

then equations (2.10) will become

$$\frac{\partial v_i}{\partial \tau}+L\left(v_i\right)=-\frac{\partial \pi}{\partial y_i}. \tag{3.5}$$

Or for each of a component of a velocity vector

$$\frac{\partial v}{\partial \tau}+L\left(v\right)=-\frac{\partial \pi}{\partial y}, \tag{3.6}$$

$$\frac{\partial w}{\partial \tau}+L\left(w\right)=-\frac{\partial \pi}{\partial z}. \tag{3.7}$$

Each equation (3.6) and (3.7) is solved in two steps, for example, for (3.6) is true

$$I.\quad \frac{\tilde{v}-v^m}{\tau}+L\left(\tilde{v}\right)=-\left\langle\frac{\partial \pi^m}{\partial y}\right\rangle. \tag{3.8}$$

$$II.\ \frac{v^{m+1}-v^m}{\tau}+L\left(\tilde{v}\right)=-\left\langle\frac{\partial \pi^{m+1}}{\partial y}\right\rangle. \tag{3.9}$$

Here $\left\langle\frac{\partial \pi}{\partial y}^m\right\rangle$ – some differenced analogue of pressure derivative. From (3.8) and (3.9) it follows

$$v^{m+1}=\tilde{v}-\tau\left\langle\frac{\partial\left(\pi^{m+1}-\pi^m\right)}{\partial y}\right\rangle. \tag{3.10}$$

In a similar way, applying procedure (3.8) - (3.9) to the equation (3.7), it is easy to receive

$$w^{m+1}=\tilde{w}-\tau\left\langle\frac{\partial\left(\pi^{m+1}-\pi^m\right)}{\partial z}\right\rangle. \tag{3.11}$$

Now, differentiating the equations (3.10) and (3.11) on y and z accordingly, and putting the received result, it is possible to receive the equation for the required correction to pressure $\delta\pi=\pi^{m+1}-\pi^m$

$$\left\langle\frac{\partial v^{m+1}}{\partial y}\right\rangle+\left\langle\frac{\partial w^{m+1}}{\partial z}\right\rangle=\left\langle\frac{\partial \tilde{v}}{\partial y}\right\rangle+\left\langle\frac{\partial \tilde{w}}{\partial z}\right\rangle-\tau\left\langle\frac{\partial^2\left(\delta\pi\right)}{\partial y^2}\right\rangle-\tau\left\langle\frac{\partial^2\left(\delta\pi\right)}{\partial z^2}\right\rangle. \tag{3.12}$$

Considering that a liquid is incompressible, on each time step the equation (2.9) should be carried out, that is it is fair

$$\left\langle \frac{\partial v^{m+1}}{\partial y} \right\rangle + \left\langle \frac{\partial w^{m+1}}{\partial z} \right\rangle = 0. \tag{3.13}$$

Consequently, from (3.12) it follows

$$\left\langle \frac{\partial^2 (\delta\pi)}{\partial y^2} \right\rangle + \left\langle \frac{\partial^2 (\delta\pi)}{\partial z^2} \right\rangle = \frac{1}{\tau} \left[\left\langle \frac{\partial \tilde{v}}{\partial y} \right\rangle + \left\langle \frac{\partial \tilde{w}}{\partial z} \right\rangle \right]. \tag{3.14}$$

It is the required Poisson equation for the correction to pressure.

Thus, the solution algorithm of initial system of the equations is following (calculation of unknown values on a time layer $t = t_{m+1}$ on known values of functions on m - th layer $t = t_m$.):

1. Components of velocity are defined from a parity of type (3.8) $\widetilde{v}$ *and* $\tilde{w}$.
2. A correction to pressure $\delta\pi$ is defined from Poisson equation (3.14).
3. Precise values of velocity $v^{m+1}$and $w^{m+1}$are defined from formulas (3.10) and (3.11).
4. A value of density $\bar{\rho}^{m+1}$ is defined from the equation (2.11).

4. Approximation of the Initial Equations

Detailed enough discussion of a question of differenced operator L entered by the formula (3.4) approximation, has been lead in work [5].

There it has noted been, that for problems of considered type when it is required descriptions of flows which contain strong heterogeneity, are required differenced schemes possessing a greater stock of stability and having good properties of monotony and dissipation.

As shown in a lot of works [4-8, 10-12], such properties compact upwind approximations of the raised accuracy (above the second order) possess. In work [8] the algorithm based on approximation both convective, and diffusion terms of Navier-Stokes equations with the third order of accuracy is realized.

At the same time, it is simple enough to generalize this algorithm on a case when diffusion terms of Navier-Stokes equations are considered even more precisely - with the fourth order of approximation.

For this purpose operator L set according to (3.4)

$$L(f) = \frac{\partial fv}{\partial y} + \frac{\partial fw}{\partial z} - \frac{1}{Re}\frac{\partial^2 f}{\partial y^2} - \frac{1}{Re}\frac{\partial^2 f}{\partial z^2} + \frac{\bar{\rho}}{Fr^2}\frac{g_i}{g}. \tag{4.1}$$

It is necessary to present it in the form of

$$Lf = L_y f + L_z f + \frac{\bar{\rho}}{Fr^2}\frac{g_i}{g}. \tag{4.2}$$

The differenced approximation of the given operator is spent as follows. For example, the following approach is applied to operator L_y

$$\langle L_y f_h \rangle = A_y^{-1}\Delta_y u f - \frac{1}{Re}B_y^{-1}\Delta_{2y} f + O\left(h^3 + \frac{h^4}{Re}\right), \tag{4.3}$$

where approximation of the second derivative is carried out with the fourth order of accuracy

$$r = \left\langle \frac{\partial^2 f}{\partial y^2} \right\rangle_h = B_y^{-1}\Delta_{2y} f = \frac{\partial^2 f}{\partial y^2} + O\left(h^4\right). \tag{4.4}$$

Operators B_y and Δ_{2y} have a following appearance:

$$B_y f = \left(E + \frac{1}{12}\Delta_2\right) f = f_i + \frac{1}{12}\left(f_{i+1} - 2f_i + f_{i-1}\right) = \frac{1}{12}f_{i-1} + \frac{10}{12}f_i + \frac{1}{12}f_{i+1},$$

$$\Delta_{2y} f = \frac{1}{h^2}\left(f_{i+1} - 2f_i + f_{i-1}\right).$$

And, according to (4.4)

$$B_y r = \Delta_{2y} f. \tag{4.5}$$

The convective terms approximation is carried out by pair of three-point operators

$$\left\langle \frac{\partial f}{\partial y} \right\rangle_h = A_y^{-1}\Delta_y f = \frac{\partial f}{\partial y} + O\left(h^3\right). \tag{4.6}$$

Entered differenced operators are introduced under following formulas:

$$A_y f = \left(A_0 - \frac{s}{4}\Delta_0\right) f; \quad \Delta_y f = \frac{1}{2h}\left(\Delta_0 - s\Delta_2\right) f.$$

Differenced operators A_0, Δ_0 and Δ_2 have a following appearance

$$A_0 f_i = \frac{1}{6}f_{i-1} + \frac{4}{6}f_i + \frac{1}{6}f_{i+1},$$

$$\Delta_0 f_i = f_{i+1} - f_{i-1},$$
$$\Delta_2 f_i = f_{i+1} - 2f_i + f_{i-1},$$

As s undertakes $s = signV$.

Consequently, applying compact upwind differences (4.3), (4.4), (3,6) to the equations (2.9) - (2.11), in the form of (3.5) it is possible to receive the differenced scheme of the solution. So, for velocity component v from the equation (3.6) the following parity turns out

$$\frac{v - v^m}{\tau} + L_y(v) + L_z(v) = -\nabla_y p^m. \tag{4.7}$$

If to enter a designation (4.8) then (4.7) will become (4.9) - (4.10) as it will be fair

$$v = v^m + \tau\epsilon,$$
$$\epsilon = \frac{v - v^m}{\tau}, \tag{4.8}$$
$$E\epsilon + L_y(v^m + \tau\epsilon) + L_z(v^m + \tau\epsilon) = -\nabla_y p^m, \tag{4.9}$$
$$E\epsilon + \tau L_y(\epsilon) + \tau L_z(\epsilon) = \phi^m, \tag{4.10}$$
$$\phi^m = -L_y(v^m) - L_z(v^m) - \nabla_y p^m. \tag{4.11}$$

Parities (4.10) - (4.11) are convenient for presenting in the form of

$$[E + \tau L_y + \tau L_z]\,\epsilon = \phi^m. \tag{4.12}$$

Last parity supposes factorization (with a margin error (τ^2)):

$$[E + \tau L_y]\,[E + \tau L_z]\,\epsilon = \phi^m. \tag{4.13}$$

The received equation is solved in two steps: the new variable is entered

$$\omega = [E + \tau L_y]\,\epsilon, \tag{4.14}$$

and concerning it the equation (4.13) which have become (4.15) is solved

$$[E + \tau L_z]\,\omega = \phi^m. \tag{4.15}$$

After definition from (4.15) value of ω there is a required value (4.8) ϵ from a parity (4.14) and further - a variable v. In more detail procedure of calculation of unknown value looks as follows. In view of that

$$L_z f = A_z^{-1}\Delta_z w f - \frac{1}{Re} B_z^{-1}\Delta_{2z} f,$$

$$L_y f = A_y^{-1}\Delta_y v f - \frac{1}{Re} B_y^{-1}\Delta_{2y} f.$$

The equations (4.14) and (4.15) will look like

$$\left[E + \tau A_z^{-1}\Delta_z w - \frac{\tau}{Re} B_z^{-1}\Delta_{2z}\right]\omega = \phi^m, \tag{4.16}$$

$$\left[E + \tau A_y^{-1}\Delta_y v - \frac{\tau}{Re} B_y^{-1}\Delta_{2y}\right]\epsilon = \omega. \tag{4.17}$$

Now, with the account of a parity (4.5), from (4.16) follows (4.18) - (4.19)

$$\left[A_z + \tau\Delta_z w\right]\omega - \frac{\tau}{Re} A_z\vartheta = A_z\left[\phi^m\right], \tag{4.18}$$

$$\Delta_{2z}\omega - B_z\vartheta = 0. \tag{4.19}$$

The received parities can be represented in a matrix type

$$\begin{pmatrix} [A_z + \tau\Delta_z w] & -\frac{\tau}{Re}A_z \\ \Delta_{2z} & -B_z \end{pmatrix}\begin{pmatrix} \omega \\ \vartheta \end{pmatrix} = \begin{pmatrix} A_z\left[\phi^m\right] \\ 0 \end{pmatrix}. \tag{4.20}$$

And if enter designations

$$G = \begin{pmatrix} [A_z + \tau\Delta_z w] & -\frac{\tau}{Re}A_z \\ \Delta_{2z} & -B_z \end{pmatrix};\ \overrightarrow{x} = \begin{pmatrix} \omega \\ \vartheta \end{pmatrix};\ \overrightarrow{f} = \begin{pmatrix} A_z\left[\phi^m\right] \\ 0 \end{pmatrix}, \tag{4.21}$$

that will turn out following system of the linear equations

$$G\overrightarrow{x} = \overrightarrow{f}, \tag{4.22}$$

with known matrix G and a vector of the right part $\overrightarrow{f}$. As all operators A and Δ, as shown above, are calculated on a three-dot pattern then matrix G will have a three-diagonal structure and, consequently, a parity (4.22) may be represented in each point of differenced grids ω_h in a following type

$$A_j\overrightarrow{x}_{j-1} + B_j\overrightarrow{x}_{j+1} - C_j\overrightarrow{x}_j = \overrightarrow{f}_j\,, \qquad j = 2, \ldots, N-1. \tag{4.23}$$

Apparently, to the received equations it is necessary to add the boundary conditions:

$$\overrightarrow{x}_1 = \Psi_1\overrightarrow{x}_2 + \overrightarrow{\mu}_1,$$
$$\overrightarrow{x}_N = \Psi_N\overrightarrow{x}_{N-1} + \overrightarrow{\mu}_N.$$

The received system of the equations is solved by a method of vector prorace [16] which is in detail considered in work [8].

After definition of value ω, from system of the equations (4.23) method described above defines unknown value from the equation (4.17).

5. Results of Calculations

By means of the offered algorithm it has been carried out numerical research of a discussed above problem about evolution of the mixed liquid ("spot"). The given results of calculations belong to a case when Brent-Vaisala period was 30 minutes, and spot radius – 10 m. Frud's number thus equaled $Fr = 1$, and the range of number of Reynolds varied from $3 \cdot 10^2$ to $3 \cdot 10^5$.

The distribution of velocity component $v(y)$ on axis of "spot" $(z = 0)$ in time moments $t = 3$, $t = 6$, $t = 9$, $t = 12$ for Reynolds's number $Re = 3 \cdot 10^2$ is presented on Figures 1-4. The distributions of velocity component $v(y)$ on axis of "spot" $(z = 0)$ for Reynolds's number $Re = 3 \cdot 10^5$ in time moments $t = 6, t = 12$ are represented in following two figures.

The calculated data were compared with results obtained in [8] based on the scheme of the third order of accuracy. These data show that the configuration of the horizontal flow velocity in the considered range of Reynolds number for the whole study period is monotonic. There is good agreement between the calculation results obtained by the schemes of third order accuracy, and proposed in this paper.

At an initial stage of evolution of "spot" (Figure 1) weak dependence of cross-section flow velocity on size of number of Reynolds is observed.

In following five figures distribution of vertical velocity on depth $w(z)$ is presented to various time-moment for a number of Reynolds $Re = 3 \cdot 10^2$. Here the considered flow characteristic is given both in the center of the indignant area (Figure 7, Figure 10), and in the field of the maximal amplitudes (Figure 8, Figure 9, Figure 11).

The figures shows the results of calculations performed on the proposed scheme and the scheme of the third order of accuracy [8]. These data indicate that both schemes give very similar results.

In a Figures 12-14 configurations of horizontal velocity $w(z)$ are presented at time-moments $t = 6$ and $t = 12$ in the field of the maximal amplitudes and in the center of "spot" for Reynolds's number $Re = 3 \cdot 10^5$. Very good concurrence of results of calculations for both considered differenced schemes is here too observed.

Distribution of function of density in the center of indignation and in the field of the maximal amplitudes for Reynolds's numbers $Re = 3 \cdot 10^2$ and $Re = 3 \cdot 10^5$ is shown on the Fig.15-20. As well as for already considered characteristics of the investigated flow - values of the horizontal and vertical velocities, cited data speak about monotonous behavior of function of density during all presented time interval $t \leq 12$ in all things a range of number of

Reynolds $3 \cdot 10^2 \leq Re \leq 3 \cdot 10^5$.

The following two pictures show behavior of sizes of vertical speed and density of current along horizontal axis($w\,(y)$ *and* $\bar{\rho}\,(y)$), Passing through a level of the maximal indignations of current (z=1,35). Here too in all things a range of considered number of Reynolds monotonous structures of investigated functions are observed.

6. Conclusion

The given results of calculations show, that application of compact upwind approximations of the fourth order of accuracy for diffusive terms at the description convective terms of the equations with the third order of accuracy for the solution of the initial equations gives quite satisfactory description of considered processes, containing strong heterogeneities.

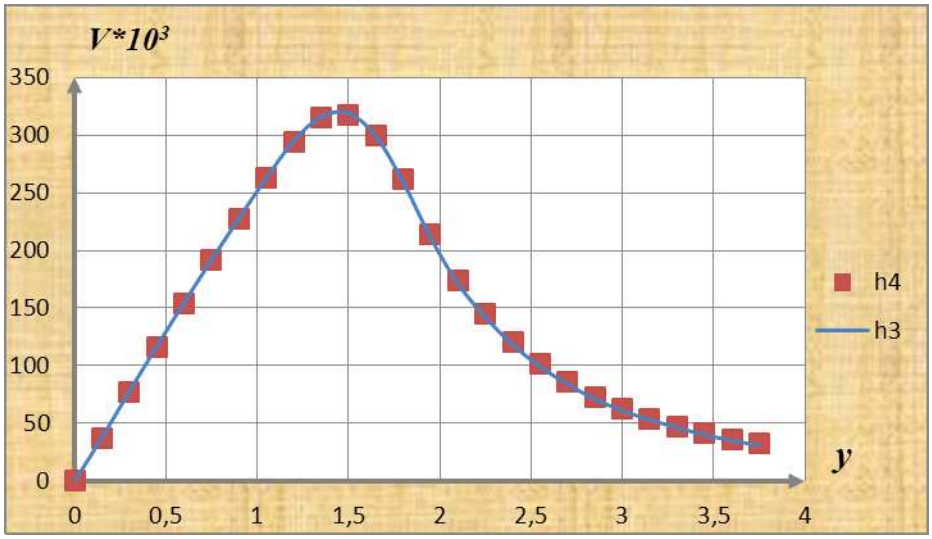

Figure 1: Graph show the horizontal velocity distribution along the Oy axis, $v(y)$ at the time moment t = 3 for Reynolds number Re = 300 in the center of spot. Solid line denotes data, obtained on scheme of third order accuracy [8], rectangular – data, obtained on scheme, considered in current paper.

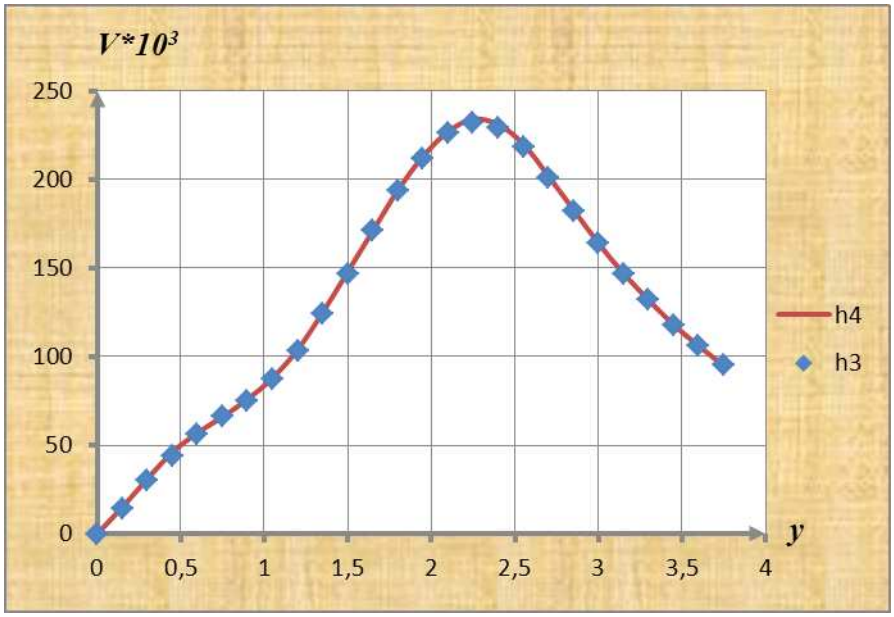

Figure 2: Graph show the horizontal velocity distribution along the Oy axis, $v(y)$ at the time moment t = 6 for Reynolds number Re = 300 in the center of spot. Solid line denotes data, obtained on scheme, considered in current paper, rectangular – data, obtained on scheme of third order accuracy [8].

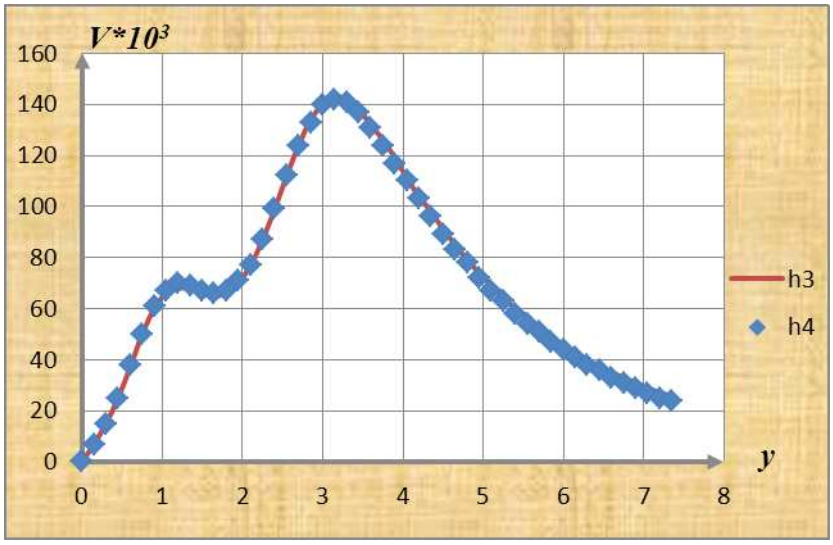

Figure 3: Graph show the horizontal velocity distribution along the Oy axis, $v(y)$ at the time moment t = 9 for Reynolds number Re = 300 in the center of spot. Solid line denotes data, obtained on scheme of third order accuracy [8], rectangular – data, obtained on scheme, considered in current paper.

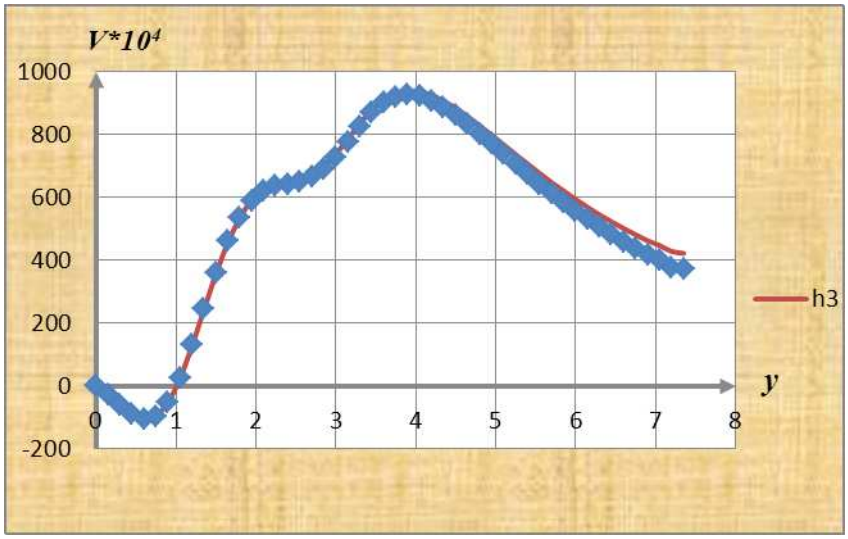

Figure 4: Graph show the horizontal velocity distribution along the Oy axis, $v(y)$ at the time moment t = 12 for Reynolds number Re = 300 in the center of spot. Solid line denotes data, obtained on scheme of third order accuracy [8], rectangular – data, obtained on scheme, considered in current paper.

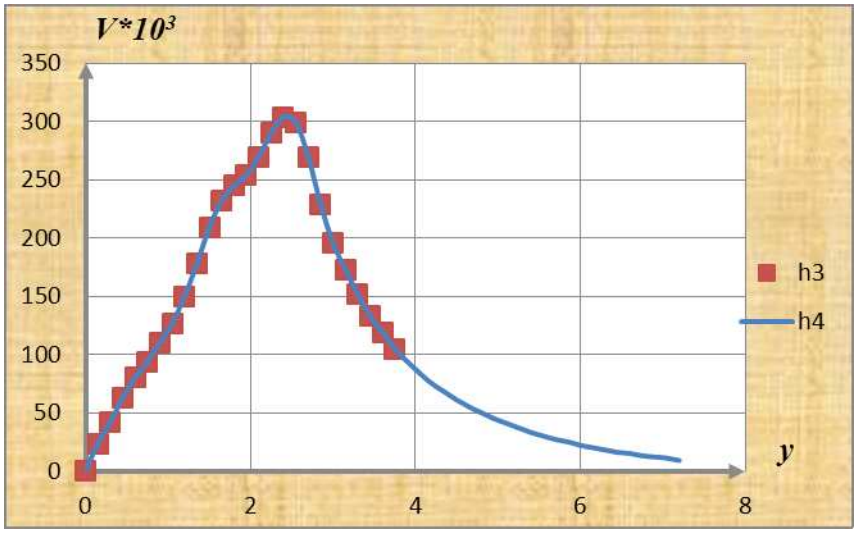

Figure 5: Graph show the horizontal velocity distribution along the Oy axis, $v(y)$ at the time moment t = 6 for Reynolds number Re = 310^5 in the center of spot. Solid line denotes data, obtained on scheme, considered in current paper, rectangular – data, obtained on scheme of third order accuracy [8].

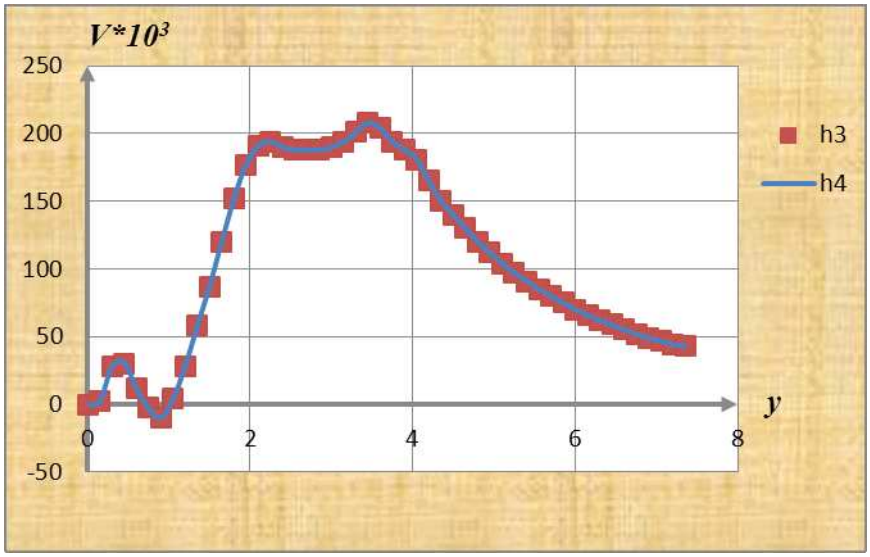

Figure 6: Graph show the horizontal velocity distribution along the Oy axis, $v(y)$ at the time moment t = 12 for Reynolds number Re = 310^5 in the center of spot. Solid line denotes data, obtained on scheme, considered in current paper, rectangular – data, obtained on scheme of third order accuracy [8].

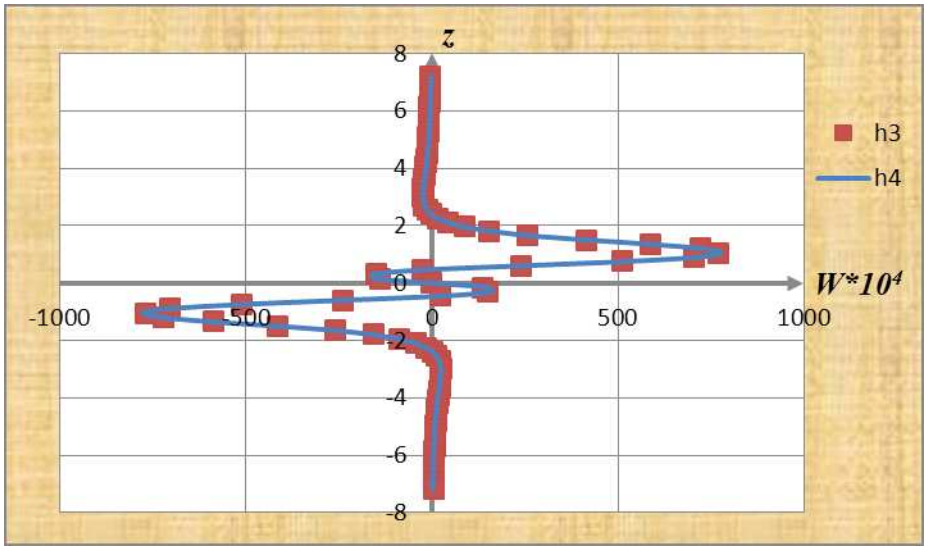

Figure 7: Graph show the vertical velocity distribution along the Oz axis, $w(z)$ at the time moment t = 6 for Reynolds number Re = 310^2 in the center of spot. Solid line denotes data, obtained on scheme, considered in current paper, rectangular – data, obtained on scheme of third order accuracy [8].

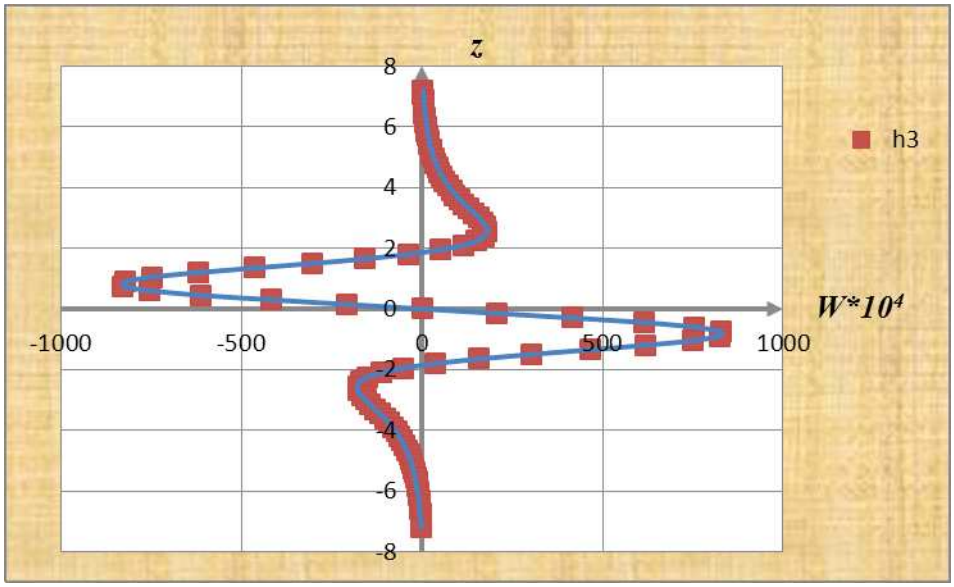

Figure 8: Graph show the vertical velocity distribution along the Oz axis, $w(z)$ at the time moment t = 6 for Reynolds number Re = 310^2 in the region of maximum amplitudes. Solid line denotes data, obtained on scheme, considered in current paper, rectangular – data, obtained on scheme of third order accuracy [8].

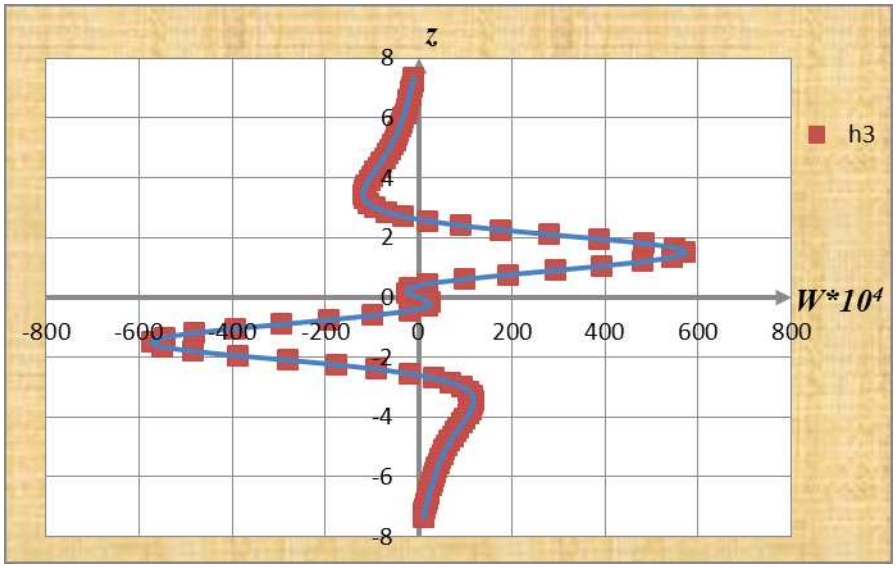

Figure 9: Graph show the vertical velocity distribution along the Oz axis, $w(z)$ at the time moment t = 9 for Reynolds number Re = 310^2 in the region of maximum amplitudes. Solid line denotes data, obtained on scheme, considered in current paper, rectangular – data, obtained on scheme of third order accuracy [8].

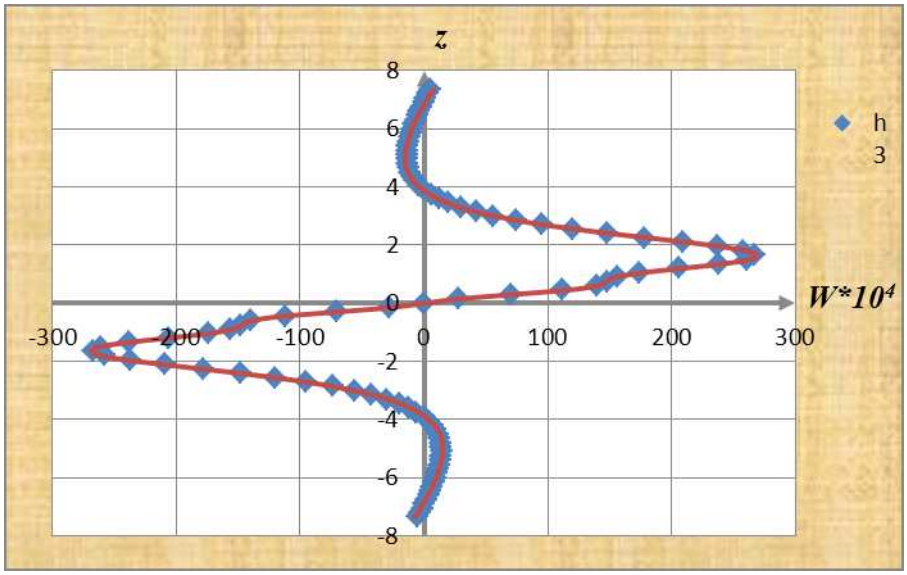

Figure 10: Graph show the vertical velocity distribution along the Oz axis, $w(z)$ at the time moment t = 12 for Reynolds number Re = 310^2 in the center of spot. Solid line denotes data, obtained on scheme, considered in current paper, rectangular – data, obtained on scheme of third order accuracy [8].

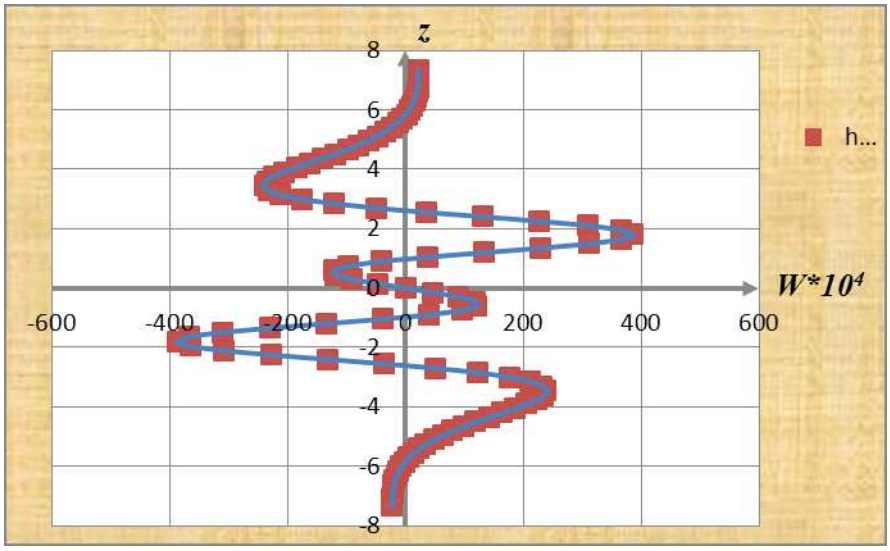

Figure 11: Graph show the vertical velocity distribution along the Oz axis, $w(z)$ at the time moment t = 12 for Reynolds number Re = 310^2 in the region of amplitudes. Solid line denotes data, obtained on scheme, considered in current paper, rectangular – data, obtained on scheme of third order accuracy [8].

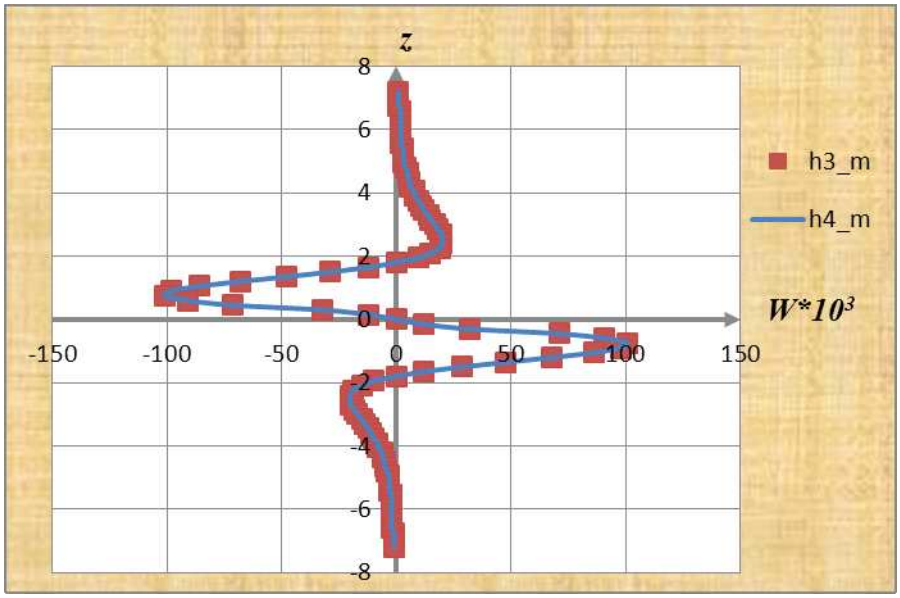

Figure 12: Graph show the vertical velocity distribution along the Oz axis, $w(z)$ at the time moment t = 6 for Reynolds number Re = 310^5 in the region of amplitudes. Solid line denotes data, obtained on scheme, considered in current paper, rectangular – data, obtained on scheme of third order accuracy [8].

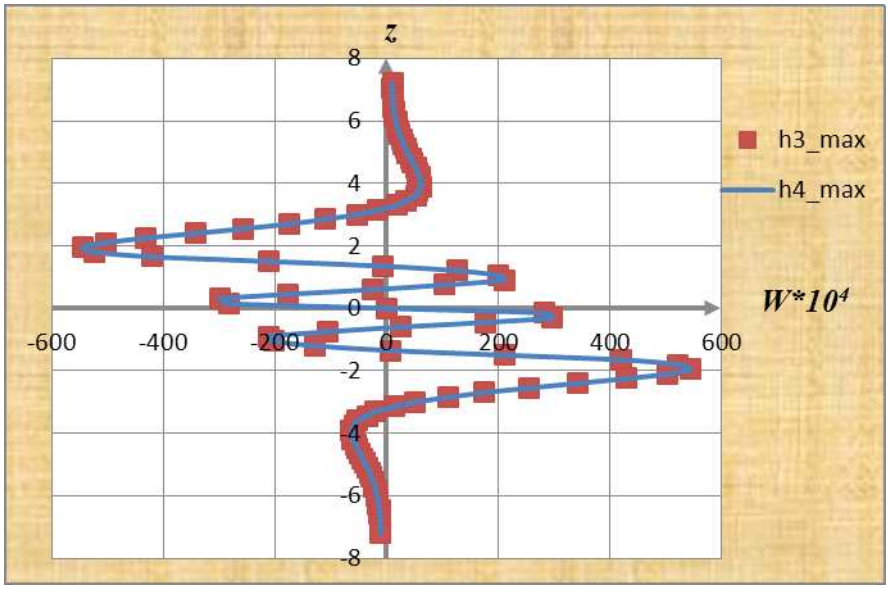

Figure 13: Graph show the vertical velocity distribution along the Oz axis, $w(z)$ at the time moment t = 12 for Reynolds number Re = 310^5 in the region of amplitudes. Solid line denotes data, obtained on scheme, considered in current paper, rectangular – data, obtained on scheme of third order accuracy [8].

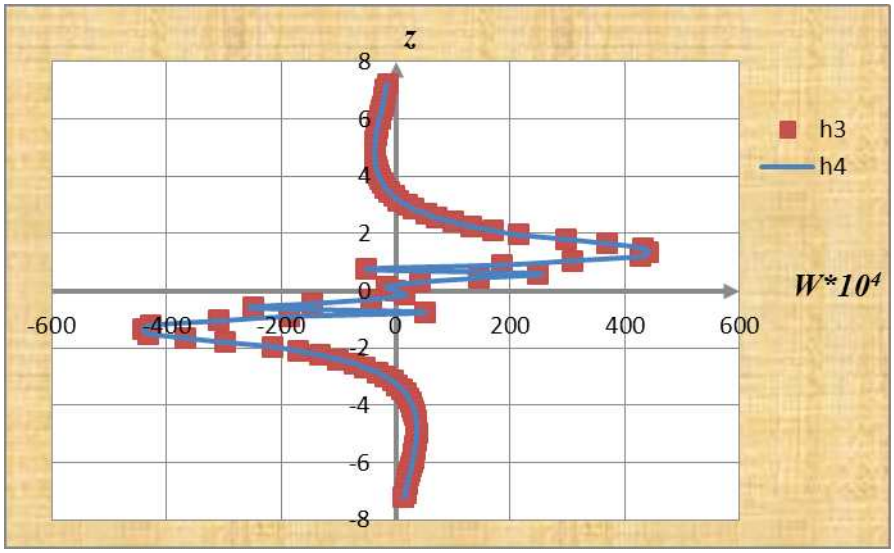

Figure 14: Graph show the vertical velocity distribution along the Oz axis, $w(z)$ at the time moment t = 12 for Reynolds number Re = 310^5 in the center of Solid line denotes data, obtained on scheme, considered in current paper, rectangular – data, obtained on scheme of third order accuracy [8].

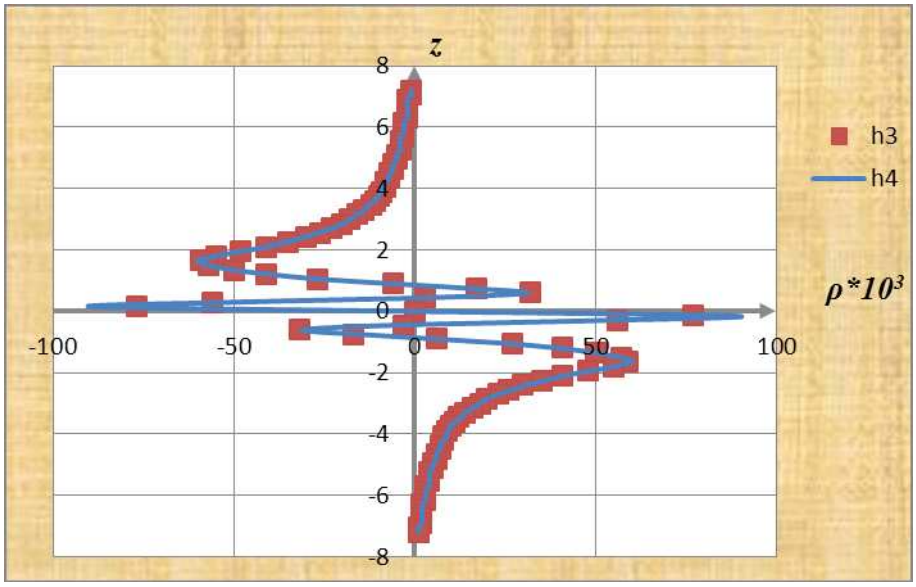

Figure 15: Graph show the density distribution along the Oz axis, $\rho(z)$at the time moment t = 6 for Reynolds number Re = 310^2 in the center of spot. Solid line denotes data, obtained on scheme, considered in current paper, rectangular – rectangular – data, obtained on scheme of third order accuracy [8].

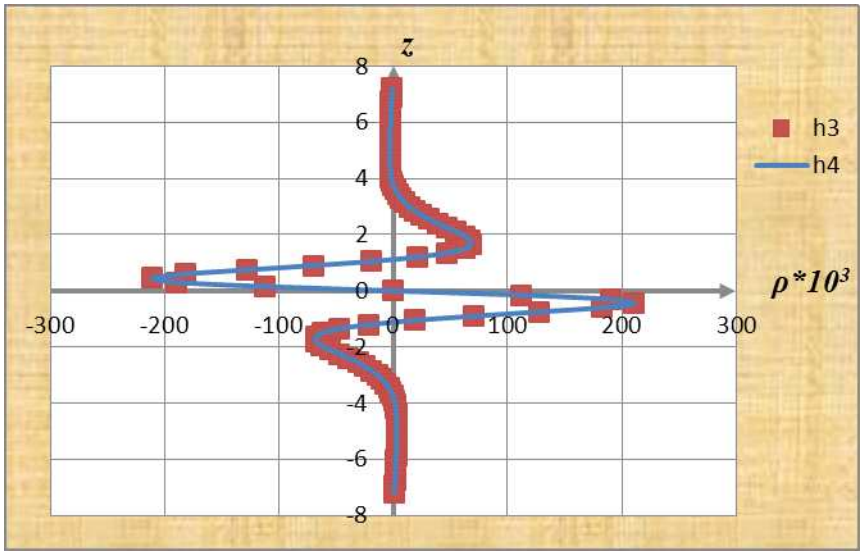

Figure 16: Graph show the density distribution along the Oz axis, $\rho(z)$at the time moment t = 6 for Reynolds number Re = 310^2 in the region of maximum amplitudes. Solid line denotes data, obtained on scheme, considered in current paper, rectangular – data, obtained on scheme of third order accuracy [8].

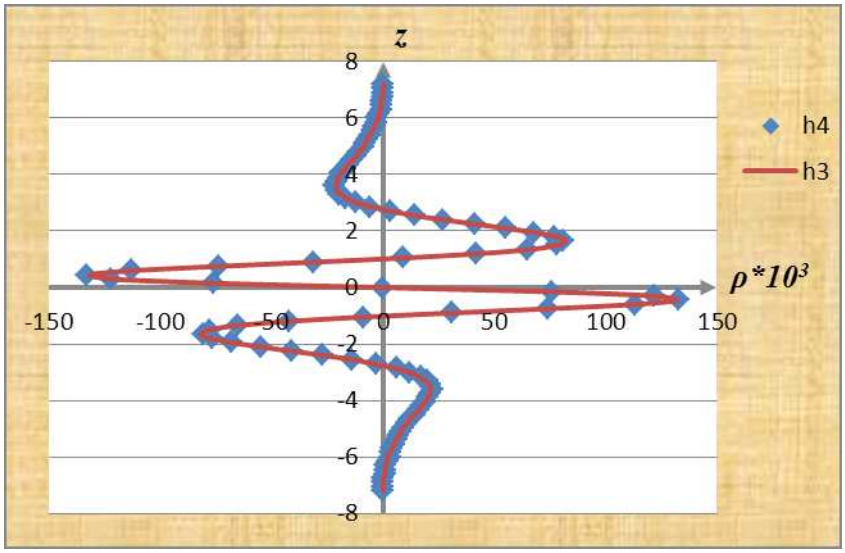

Figure 17: Graph show the density distribution along the Oz axis, $\rho(z)$at the time moment t = 9 for Reynolds number Re = 310^2 in the region of maximum amplitudes. Solid line denotes data, obtained on scheme of third order accuracy [8], rectangular – data, obtained on scheme considered in current paper.

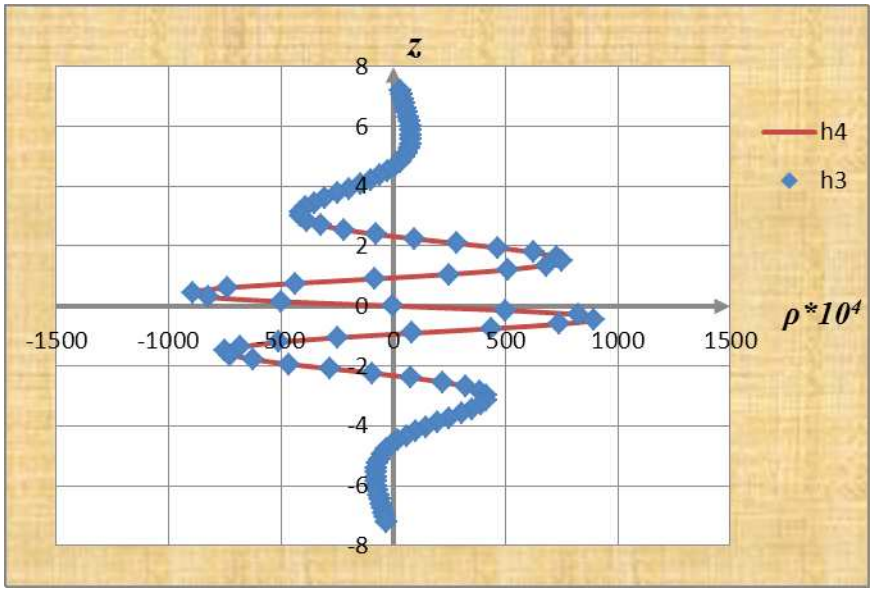

Figure 18: Graph show the density distribution along the Oz axis, $\rho(z)$at the time moment t = 12 for Reynolds number Re = 310^2 in the region of maximum amplitudes. Solid line denotes data, obtained on scheme, considered in current paper, rectangular – data, obtained on scheme of third order accuracy [8].

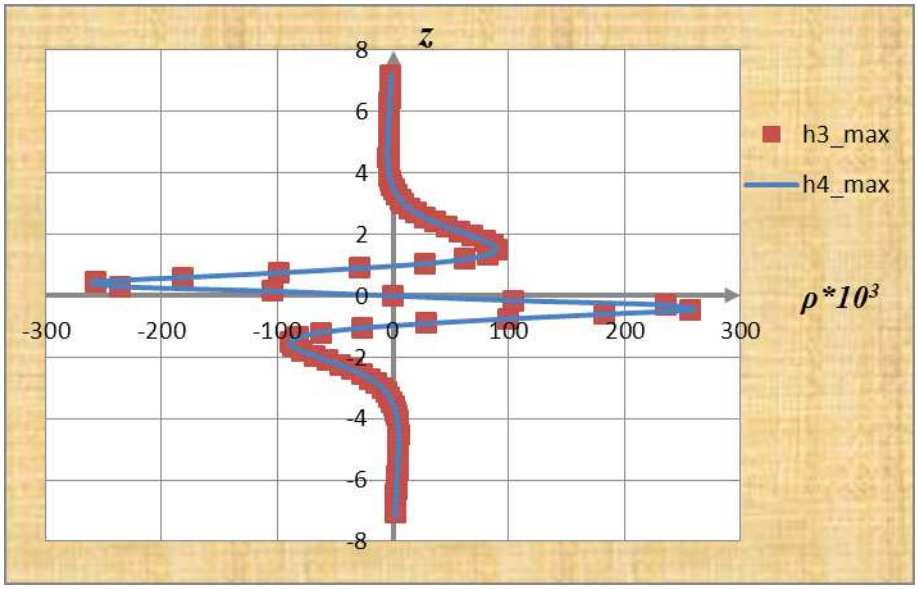

Figure 19: Graph show the density distribution along the Oz axis, $\rho(z)$at the time moment t = 6 for Reynolds number Re = 310^5 in the region of maximum amplitudes. Solid line denotes data, obtained on scheme, considered in current paper, rectangular – data, obtained on scheme of third order accuracy [8].

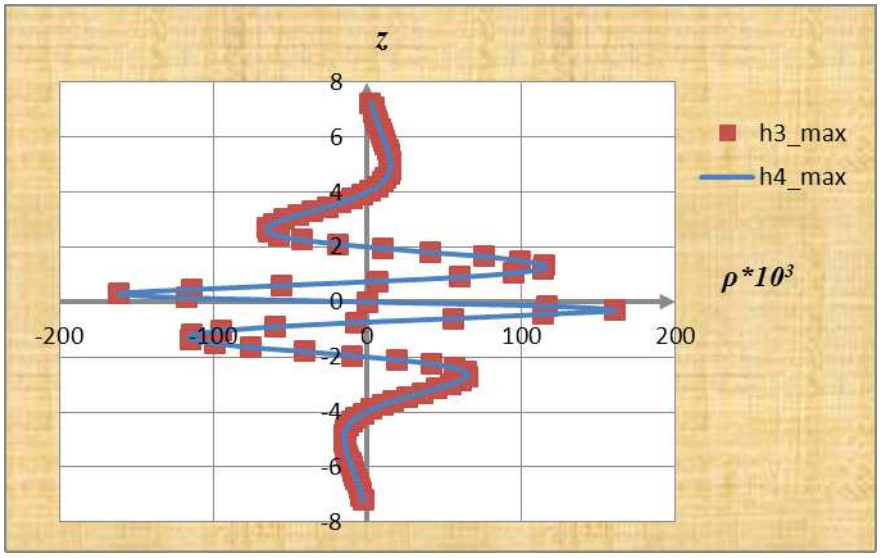

Figure 20: Graph show the density distribution along the Oz axis, $\rho(z)$ at the time moment t = 12 for Reynolds number Re = 310^5 in the region of maximum amplitudes. Solid line denotes data, obtained on scheme, considered in current paper, rectangular – data, obtained on scheme of third order accuracy [8].

References

[1] F. Harlow, J. Welch, Numerical calculation of time-dpendent viscous incompressible flow of fluid with free surface, *Physics of Fluids*, **8**, No. 12 (1965), 2182-2189.

[2] O.M. Belotserkovsky, V.A. Guschin, V.V. Schennikov, Splitting method in application to the solution of problems of dynamics of viscous incompressible liquid, *J. Comput. Math. and Math. Phys.*, **15**, No. 1 (1975), 197-207, In Russian.

[3] A.Y. Danilenko, V.I. Kostin, A.I. Tolstykh, *The Implicit Algorithm of Calculating Currents of a Homogeneous and Non-Homogeneous Fluid*, M., Dorodnicyn Computing Center, USSR Academy of Sciences (1985), In Russian.

[4] V.I. Kostin, *Numerical Modeling of Some Problems of Oceanology on the Basis of the Compact Schemes of Third Order*, M., Dorodnicyn Computing Center, USSR Academy of Sciences (1991), In Russian.

[5] V.I. Kostin, Application of compact approximations of the third order to address some of the tasks of an inhomogeneous incompressible fluid, In: *Proceedings of the XV Conference of Young Scientists*, MIPT, Moscow, (1990); Part 1 of the article, DEP. In VINITI, No. 6174, 135-148, In Russian.

[6] A.N. Kopysov, V.I. Kostin, Sound radiation of turbulent jet in the wake flow at small Mach numbers, In: *Proceedings of the XV Conference of Young Scientists*, MIPT, Moscow, (1990); Part 1 of the article, DEP, In VINITI, No. 6174, 120-134, In Russian.

[7] A.N. Kopysov, V.I. Kostin, *Numerical Simulation of Sound Emission Turbulent Flow in a Stratified Medium*, Moscow, Dorodnicyn Computing Center, USSR Academy of Sciences (1991), In Russian.

[8] V.I. Kostin, On one method of calculating currents of a viscous incompressible fluid, *River Transport (XXI Century)*, **52**, No. 4 (2011), 64-70, In Russian.

[9] V.V. Rykov, *Numerical Modeling of Spatial Flows of Incompressible Viscous Fluid*, Moscow, Dorodnicyn Computing Center, USSR Academy of Sciences (1983), In Russian.

[10] A.I. Tolstykh, *Compact Difference Schemes and their Application in Problems of Aerohydrodynamics*, Moscow, Nauka (1990), In Russian.

[11] A.I. Tolstykh, Development of arbitrary-ordermultioperators-basedschemes forparallel calculations. 1: Higher-than-fifth-order approximations to convection terms, *J. Comput. Phys.*, **225** (2007), 2333-2353.

[12] M.V. Lipavskii, A.I. Tolstykh, E.N. Chigirev, A parallel computational scheme with ninth-order multioperator approximations and its application to direct numerical simulation, *Comput. Math., Math. Phys.*, **46**, No. 8 (2006), 1433-1452 (Transl. from Russian).

[13] A.S. Monin, A.M. Yaglom, *Statistical Hydromechanics*, Part 1, Moscow, Nauka (1964), In Russian.

[14] N.E. Cochin, I.A. Kibel, N.V. Rose, *Theoretical Hydromechanics*, Parts 1, 2, Moscow, Physmathgiz (1963), In Russian.

[15] *Oceanology, Physics of the Ocean*, Volume 1: Hydrophysics of the Ocean (Ed. A.S. Monin), Moscow, Nauka (1978), In Russian.

[16] A.A Samarsky, E.S. Nikolaev, *Methods of the Decision of the Grid Equations*, Moscow, Nauka (1978), In Russian.